Classification of composite damage from FBG load monitoring signals

Aydin Rajabzadeh, Richard C. Hendriks, Richard Heusdens, Roger M. Groves

Aydin Rajabzadeh, Richard C. Hendriks, Richard Heusdens, Roger M. Groves, "Classification of composite damage from FBG load monitoring signals," Proc. SPIE 10168, Sensors and Smart Structures Technologies for Civil, Mechanical, and Aerospace Systems 2017, 1016831 (12 April 2017); doi: 10.1117/12.2257660

SPIE.

Event: SPIE Smart Structures and Materials + Nondestructive Evaluation and Health Monitoring, 2017, Portland, Oregon, United States

Classification of composite damage from FBG load monitoring signals

Aydin Rajabzadeh[a,b], Richard C. Hendriks[a], Richard Heusdens[a], and Roger M. Groves[b]

[a]Circuits and Systems Group, Faculty of Electrical Engineering, Mathematics and Computer Science, Delft University of Technology, Mekelweg 4, 2628 CD Delft, The Netherlands
[b]Aerospace Non-Destructive Testing Laboratory, Faculty of Aerospace Engineering, Delft University of Technology, Kluyverweg 1, 2600 GB Delft, The Netherlands

ABSTRACT

This paper describes a new method for the classification and identification of two major types of defects in composites, namely delamination and matrix cracks, by classification of the spectral features of fibre Bragg grating (FBG) signals. In aeronautical applications of composites, after a damage is detected, it is very useful to know the type of damage prior to determining the treatment method of the area or perhaps replacing the part. This was achieved by embedding FBG sensors inside a glass-fibre composite, and analysing the output signal from the sensors. The glass-fibre coupons were subjected to mode-I loading under tension-compression and static tests, in order to induce matrix cracks and delamination damages respectively. Afterwards, using wavelet features extracted from spectral measurements of the FBG sensors, classification of the damage type was carried out by means of support vector machines as a general classification tool with a quadratic kernel.

Keywords: Fibre Bragg grating (FBG), load monitoring, delamination, matrix crack, classification, support vector machines (SVM), wavelet features

1. INTRODUCTION

One of the main purposes of structural health monitoring (SHM) is to detect and identify usually adverse changes in materials[1] . For the case of composites in particular, several methods have already been developed that have the potential to successfully detect these changes. However, many of these methods need human supervision to perform the data acquisition, and sometimes to interpret the acquired data as well. On the other hand, embedded fibre Bragg grating (FBG) sensors are increasingly utilised in SHM applications of materials[2,3] and potentially, they have the capability of being interrogated automatically. In addition, since they have multiplexing capabilities, multiple FBG sensors can be interrogated at the same time[4] , which can result in a larger inspection area.

There has been several papers in the past few decades in the literature on the application of FBG sensors in SHM. In some of these papers analysis of the dynamic or static changes in the Bragg wavelength is being studied, which supposably contains information about the location of the damage and its type. Frieden et al. proposed a method for localisation and detection of damage based on the dynamic changes in the Bragg wavelength of FBG sensors in response to the propagated lamb waves in composites[5] . Loutas et al. used the dynamic strain measurements based on transient shifts in the Bragg wavelength of FBGs and pattern recognition tools in order to identify the state of the damage[6] . Lu et al. used C-SVC binary classifier and same set of information to identify the damage and also to localise it[7] . However in order to have a proper resolution for the dynamic strain measurements, it is required to have an interrogator with high full range scanning frequency. The second group of papers focuses on exploiting the full range of FBG reflected spectra. Luyckx et al. showed the effects of embedding FBGs in different composite configurations on its reflected spectra[8] . Sorensen et al. analysed the effects of non-uniform strains due to propagation of mode-I delamination damage, and its effect on the full range of FBG reflected spectra[9] . The current study belongs to the later group and the full range of FBG reflected spectra is used to identify and classify the damage.

Further author information
A.rajabzadehdizaji@tudelft.nl, R.C.Hendriks@tudelft.nl, R.Heusdens@tudelft.nl, R.M.Groves@tudelft.nl

Sensors and Smart Structures Technologies for Civil, Mechanical, and Aerospace Systems 2017, edited by Jerome P. Lynch, Proc. of SPIE Vol. 10168, 1016831 · © 2017 SPIE
CCC code: 0277-786X/17/$18 · doi: 10.1117/12.2257660

1.1 FBG Theory

An undisturbed FBG sensor with a uniform grating is a periodic modulation of the refractive index of an optical fibre's core for a certain length, usually from $1\,mm$ to $24\,mm$. There are several methods for inducing this refractive index modulation which are mostly based on exposing the core to a spatially modulated UV light radiation. These methods include using a phase mask[10] or interfering two UV laser beams[11] . When connected to a (usually) broadband light source, this length of refractive index modulation acts like a mirror for certain wavelengths and (partially) reflects them. The strain or temperature distribution along the length of the sensor is translated into alterations in this reflected spectra in wavelength domain. For a sensor that has not undergone a non-uniform strain or temperature change, the reflected spectra is strongest at a wavelength called the Bragg wavelength (λ_B), which is given by[12] :

$$\lambda_B = 2n_{eff}\Lambda \tag{1}$$

where n_{eff} is the effective refractive index of the core and Λ is the period of the grating, which is constant in a uniform modulation. Any change in axial strain or temperature along the sensor length will result in a change in the period of the grating, and therefore a shift in the Bragg wavelength. If the sensor was exposed to different strain (temperature) values along its length, then the transfer matrix method suggests the emergence of multiple peaks and an overall broadening of reflected spectrum[13] . It has been shown in the literature that different damage types result in different strain distributions along the length of the sensor[14,15] . There is a (nonlinear) relationship between these strain distributions and changes in the reflected spectra of the FBG sensors. A difference between the strain distribution of different damage types is therefore expected to also result in distinguishable reflected spectra. This paper investigates the analysis of the reflected spectra of several glass fibre composite coupons, under different static and dynamic loads. The goal of this experiment is to classify these outputs and determine the type of damage applied to the coupon automatically, with a set of features extracted from the full range of spectral graphs.

2. EXPERIMENT DESIGN

The focus of this study is on the effect of two different types of loading on glass fibre composites. In the first scenario, mode-I static loading with opening orthogonal to the fibre direction was applied on the composite samples with an initial induced opening. The FBG sensors were embedded in the middle layer of the composites during production. These already partially defected specimens were then put inside a $10\,kN$ static loading machine. The second scenario was designed to induce matrix cracks in the specimens, by subjecting them to mode-I fatigue loading orthogonal to the direction of the fibres. The specimens (with embedded FBGs) were then subjected to a tension/compression test in a $100\,kN$ fatigue machine.

2.1 FBG sensors and interrogation equipment

For this study eight draw tower grating (DTG) sensors (from the company FBGS) were used. The length of optical fibres was about 1 meter (excluding the connectors), and the gratings were 8 mm long with peak wavelengths distributed in the range of $1530\,nm$ to $1570\,nm$. Four sensors were used for each class of defects. Interrogation of the sensors was performed by the NI-PXIe 4844 optical sensor interrogator (National Instruments). This interrogator has wavelength accuracy of $4\,pm$ and can cover the wavelength range of $1510\,nm$ to $1590\,nm$. The recording of the signals was carried out using LabVIEW software.

2.2 Composite production

Unidirectional glass fibres with a density of $1200\,g/cm^3$ were used for composite production, as the effect of FBG embedment in the composite is assumed to be negligible in higher density of reinforcement fibres. The composite was produced using the cold infusion method, with vacuum bagging technique. All specimens (for both tests) have the same layup of $[0_2/90_2/0_2]$, resulting in a $4.5\,mm$ thick composite panel. This layup was selected for the following reasons: The FBG sensors were needed to be embedded in the zero degree layer adjacent to 90 degree layer, so that after the tension/compression test, the matrix cracks in the 90 degree layer would be passing near or below FBG sensors so it can sense them; Also due to the high density of glass fibres sheets, adding more layers would have resulted in a very thick final product.

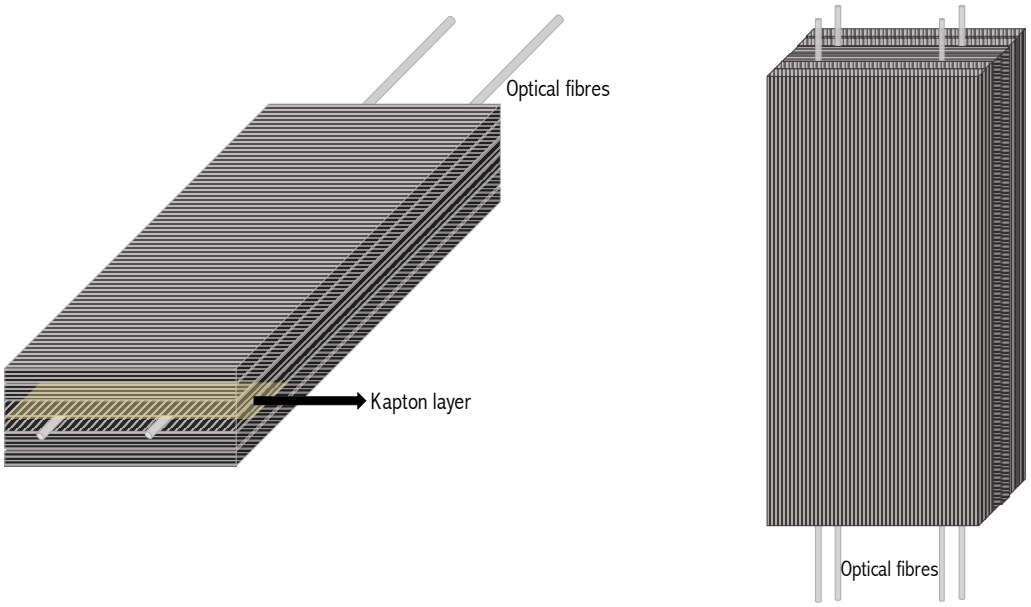

Figure 1: The specimens designed for (a) delamination tests, and (b) fatigue tests.

For the specimens designed for delamination damages, optical fibers were placed between the 3rd and 4th layer, along the length of the reinforcement fibers of the zero-degree layer, and their connector end sticking out of one end of the composite (with a protecting tube of $200\,\mu m$ internal diameter placed in the air/composite interface) and cut on the other end. The connectors were removed on the other end since only the reflected signal was going to be analysed and the transmitted signal contained no additional information. Also by removing them and creating a non-uniform cross section at the end of the fibre, the possibility of back reflection from the end of the optical fibre was eliminated. In order to induce a preliminary delamination in the "delamination" samples, a Kapton layer with width of $2\,cm$ and thickness of $20\,\mu m$ was put at the side of the composite panel between the 3rd and 4th layers. For matrix crack samples two of the optical fibers were placed between the 2nd and 3rd layer, and two of them between the 4th and 5th layers. Figure 1 shows a schematic of the specimens' configurations and the location of optical fibres inside them.
After production, the composite panels were cut into smaller coupons. For delamination tests, the size of the coupons were $5 \times 20\,cm$, and for the matrix crack tests, they were $4 \times 15\,cm$. After the production and cutting of the coupons, the output signals of FBG sensors were recorded in the wavelength domain (spectral graphs). These signals were going to be used as the reference signals for the healthy samples.

2.3 Fatigue and static tests

For the delamination test, the samples needed to be equipped with metal grips first. This was performed by using $3M^{TM}$ Scotch-Weld^{TM} EC-9323 B/A Epoxy adhesive. A $10\,kN$ MTS 810 machine was used to perform a static delamination test on the samples. In order to have more control over the speed of opening, a displacement-controlled approach was used. By increasing the displacement parameter on the controller software, there was a point where the output started to show changes. The reflected spectra were recorded at this point. Then the opening was increased in steps of $0.1\ mm$, and at each step the output was recorded. The procedure continued until there was no change in the shape of the output signal anymore. Figure 2a shows a specimen in static load test at its final opening position. After performing the test on all specimens, a database of overall 280 (unique) sample signals was acquired. In other words, 280 different full range reflected spectra were recorded, which were all associated with delamination type defects.
For the tension/compression fatigue test, paper tabs were attached on the ends of the specimens using cyanoacrylate adhesive. For this test a $100\,kN$ MTS 810 fatigue machine was used. Using a displacement controlled ap-

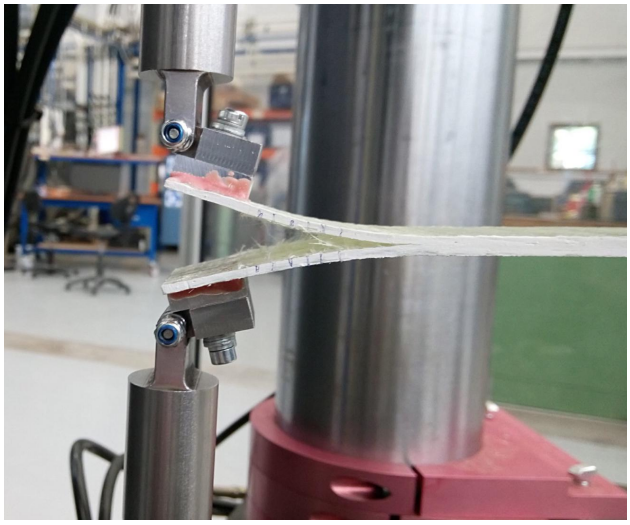

(a)

(b)

Figure 2: The specimens under (a) mode-I static loading with the opening orthogonal to the fibre direction to induce delamination type damages, and (b) mode-I fatigue loading along the fibre direction to induce matrix crack type damages.

proach (for the same reason as the delamination tests), we did the fatigue test with the offset of $0\,mm$, amplitude of $0.4\,mm$ and frequency a of $10\,Hz$. The output of sensors was recorded after each 500 cycles. After around 80000 cycles the specimen broke and the data acquisition stopped. Figure 2b shows a specimen inside a fatigue load test machine. By the end of the test, a database of 146 (unique) sample signals was acquired associated with matrix crack defects.

3. SIGNAL PROCESSING AND CLASSIFICATION

In this study the classification was based on statistical pattern recognition and classification, in which a statistical feature set extracted from the signals are input to a classifier. Support vector machines with quadratic kernels were chosen as a general classification tool for this application.

3.1 Support vector machine theory

Support vector machines (SVM) are one of the most versatile machine learning approaches in both classification and regression. For the case of linear binary classification, SVM tries to find an affine hyperplane that has a maximum distance from the nearest points of each group called support vectors[16] . When the feature set is not linearly separable, one trick to solve the problem is to map the feature set to a higher dimension, in which the new feature set is linearly separable. Kernel methods can create this mapping to higher dimensions[17] . Suppose the task is to classify a training dataset with n points of the form:

$$(x_1, y_1), (x_2, y_2), ..., (x_n, y_n), \tag{2}$$

in which the x_i's are the p-dimensional feature vectors and y_i's are the corresponding class labels that are either $+1$ or -1. The original problem without the use of the kernel method is to find the set of parameters w and b in the following classifying affine hyperplane.

$$f(x) = w^T x + b, \tag{3}$$

in which $x = [x_1, x_2, ..., x_n]^T$, and w^T (the weight vector) and b (the offset vector) are calculated by solving the optimisation problem that tries to maximise the distance between this hyperplane and the selected support vectors. Applying kernel functions on the feature space, converts the hyperplane to the following form.

$$f(x) = w^T \Phi(x) + b, \tag{4}$$

where in our case the kernel function has the following quadratic form:

$$\Phi(x) = K(x, x') = (x.x' + 1)^2 \tag{5}$$

where x and x' are vectors from the input feature space and "." operator represents the inner product between two feature vectors. Applying the kernel function on the feature set projects it to a higher dimension which makes it linearly separable by a linear SVM classifier.

3.2 Feature extraction and classification results

A length of 2000 samples ($8nm$) around the peak wavelength, with the peak wavelength in the centre, was considered as the part containing the information about the damage. Figure 3 shows an example of a selected spectral range, in which Figure 3a shows the signal before occurrence of any damage, and Figure 3b shows the output signal of the same sensor after being affected by the delamination defect. Figure 4 presents the same comparison for fatigue load damages.

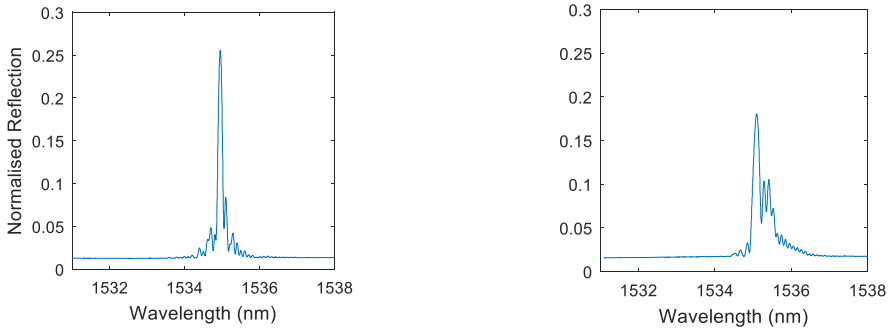

(a) (b)

Figure 3: FBG reflected spectra from: (a) a healthy specimen, and (b) from a damaged specimen by delamination.

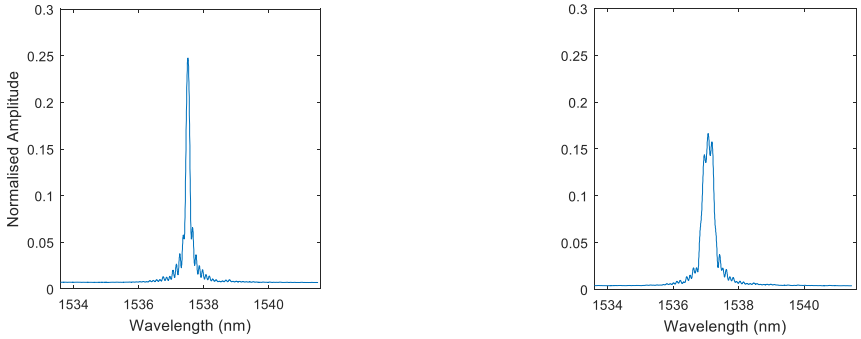

(a) (b)

Figure 4: FBG reflected spectra from: (a) a healthy specimen, and (b) from a damaged specimen by fatigue test.

A set of features were generated for these signals. For this application it was found out empirically that using statistics based on wavelet transformation of the signal leads to the highest classification accuracy. By applying

the wavelet transform and decomposing the original signal into 5 detail and 1 approximate signals (using the Daubechies 4 mother wavelet), statistical measures of the following form were extracted:

- Mean, variance, kurtosis, skewness, complexity and mobility of each subband (i.e., for each of the 5 detail signals and 1 approximate signal)
- Power of each subband
- Absolute mean value ratio of each subband and its adjacent subband (i.e. $D1/D2$, $D2/D3$, ... and $D5/A5$ in which D stands for absolute mean value of detail signals and A for absolute mean value of approximate signals).

In total this leads to 47 features for each sample data. Again the choice of mother wavelet and number of decompositions were determined empirically. An example of this wavelet decomposition on the damaged sample with fatigue error (the signal sample presented in Figure 4b) is shown in Figure 5.
In order to avoid over-parameterisation and increase generalisation, these features were later reduced to 10 of the best features using the sequential forward selection (SFS) method[18] . These features were then fed to a support vector machine (SVM) classifier with quadratic kernel. Figure 6 shows the samples with respect to two of the best features, and the designed classifier. About 75 percent of the data was used to train the classifier. The remaining data was used as the test dataset.

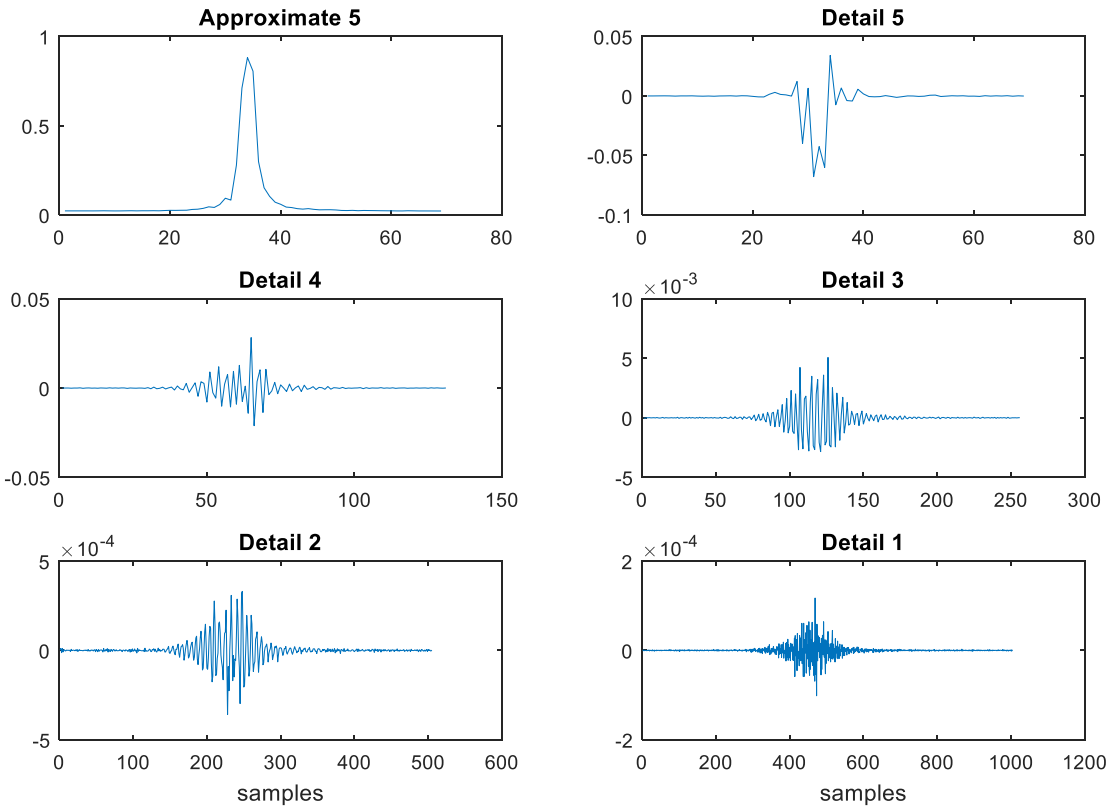

Figure 5: Wavelet decomposition of the FBG signal from one of the fatigue load specimens.

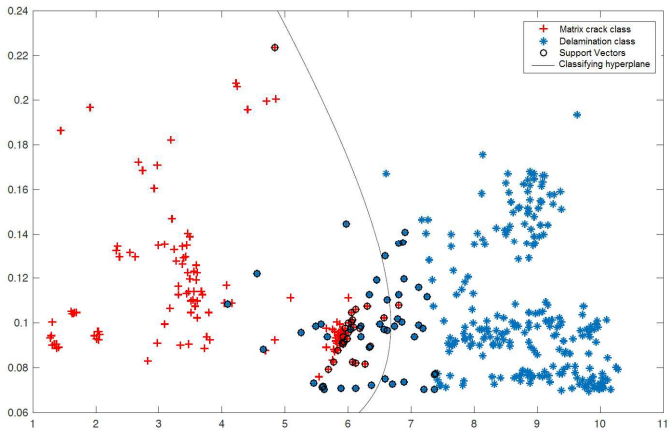

Figure 6: Classification result of the two classes, based on two of the best features in wavelet domain, including the mean values of approximate band and absolute mean value ratio of $D5/A5$.

4. DISCUSSION

An interesting result of the classification was that if the classifier was trained based on a random subset of the dataset, the classification results were very high. In fact, in this case, the classification accuracy of the test data for the "fatigue load" class was 97.2% and for the "static load" class was 93.8%. However, it was observed that the outputs also depend on the individual sensors, composite coupons, testing environment and possibly other factors as well. In order to show this dependency, the data from one of the sensors was isolated from the rest. The classifier was then trained with the dataset from the remaining 7 sensors and the dataset from the isolated sensor was used as the test data. It was observed that a drop of nearly 10% in the classification accuracy of the "delamination" class was resulted. This decrease in the classification accuracy was less severe for the "matrix crack" class, with a drop of less than 3%. In order to overcome this problem the authors either suggest increasing the dataset by including more sensors and specimens in the experiments, or to make the damaged output independent from its original shape. It has been already discussed in the literature that embedding FBGs between composite layers could impose a residual strain distribution along the length of the FBG[19–21] . Therefore there would be a bias in the results of the classifications, because of these initial conditions. It was also observed in this paper that embedding FBG sensors increases the FWHM of the signals by factors of more than four, which could also contribute to the initial bias on the output of individual FBG sensors.

5. CONCLUSIONS

The goal of this paper was to examine the possibility of classifying two major types of damages, including delamination and matrix cracks, based on the information in the reflection spectra of FBG sensors. In order to distinguish between the two classes, a set of features based on discrete wavelet transformation were extracted from each set of signals for each class, and after feature selection, they were fed to a SVM classifying machine. Classification with rather high accuracies were achieved, however it was observed that isolation of one sensor from the rest of the dataset and using it as a test data reduces this classification accuracy.

REFERENCES

[1] Farrar, C. R., and Worden K. *"Structural Health Monitoring: a Machine Learning Perspective"*. John Wiley & Sons, 2012.

[2] Shrestha, P., Kim, J. H., Park, Y., and Kim, C. G. *"Impact localization on composite structure using FBG sensors and novel impact localization technique based on error outliers"*. Composite Structures, 142, pp.263-271, 2016.

[3] Takeda, N., Okabe, Y. and Mizutani, T. *"Damage detection in composites using optical fibre sensors"*. Proceedings of the Institution of Mechanical Engineers, Part G: Journal of Aerospace Engineering, 221(4), pp.497-508, 2007.

[4] Rao, Y. J. *"In-fibre Bragg grating sensors"*. Measurement science and technology, 8(4), 355, 1997.

[5] Frieden, J., Cugnoni, J., Botsis, J., and Gmr, T. *"Low energy impact damage monitoring of composites using dynamic strain signals from FBG sensors Part I: Impact detection and localization"*. Composite Structures, 94(2), 438-445, 2012.

[6] Loutas, T. H., Panopoulou, A., Roulias, D., and Kostopoulos, V. *"Intelligent health monitoring of aerospace composite structures based on dynamic strain measurements"*. Expert Systems with Applications, 39(9), 8412-8422, 2012.

[7] Lu, S., Jiang, M., Sui, Q., Sai, Y., and Jia, L. *"Damage identification system of CFRP using fiber Bragg grating sensors"*. Composite Structures, 125, 400-406, 2015.

[8] Luyckx, G., Voet, E., Lammens, N., and Degrieck, J. *"Strain measurements of composite laminates with embedded fibre Bragg gratings: Criticism and opportunities for research"*. Sensors, 11(1), 384-408, 2010.

[9] Sorensen, L., Botsis, J., Gmr, T., and Cugnoni, J. *"Delamination detection and characterisation of bridging tractions using long FBG optical sensors"*. Composites Part A: Applied Science and Manufacturing, 38(10), 2087-2096, 2007.

[10] Hill, K. O., and Meltz, G. *"Fiber Bragg grating technology fundamentals and overview"*. Journal of lightwave technology, 15(8), 1263-1276, 1997.

[11] Bennion, I., Williams, J. A. R., Zhang, L., Sugden, K., and Doran, N. J. *"UV-written in-fibre Bragg gratings"*. Optical and Quantum Electronics, 28(2), 93-135, 1996.

[12] Kashyap, R. *"Fiber Bragg gratings"*. Academic press, 1999.

[13] Yamada, M., and Sakuda K.. *"Analysis of almost-periodic distributed feedback slab waveguides via a fundamental matrix approach"*. Applied optics, 26(16), pp.3474-3478, 1987.

[14] Okabe, Y., Yashiro, S., Kosaka, T., and Takeda, N. *"Detection of transverse cracks in CFRP composites using embedded fiber Bragg grating sensors"*. Smart Materials and Structures, 9(6), p.832, 2000.

[15] Takeda, S., Minakuchi, S., Okabe, Y., and Takeda, N. *"Delamination monitoring of laminated composites subjected to low-velocity impact using small-diameter FBG sensors"*. Composites Part A: Applied Science and Manufacturing, 36(7), pp.903-908, 2005.

[16] Cortes, C., and Vapnik, V. *"Support-vector networks"*. Machine learning, 20(3), pp.273-297, 1995.

[17] Boser, B. E., Guyon, I. M., and Vapnik, V. N. *"A training algorithm for optimal margin classifiers"*. In Proceedings of the fifth annual workshop on Computational learning theory (pp. 144-152). ACM, 1992.

[18] Pudil, P., Novovicova, J., and Kittler, J. *"Floating search methods in feature selection"*. Pattern recognition letters, 15(11), pp.1119-1125, 1994.

[19] Colpo, F., Humbert, L., Giaccari, P., and Botsis, J. *"Characterization of residual strains in an epoxy block using an embedded FBG sensor and the OLCR technique"* Composites Part A: Applied Science and Manufacturing, 37(4), 652-661, 2006.

[20] Okabe, Y., Yashiro, S., Tsuji, R., Mizutani, T., and Takeda, N *"Effect of thermal residual stress on the reflection spectrum from fiber Bragg grating sensors embedded in CFRP laminates"* Composites Part A: Applied Science and Manufacturing, 33(7), 991-999, 2002.

[21] Botsis, J., Humbert, L., Colpo, F., and Giaccari, P. *"Embedded fiber Bragg grating sensor for internal strain measurements in polymeric materials"* Optics and lasers in Engineering, 43(3), 491-510, 2005.